Electronic Supplementary Material (ESI) for Lab on a Chip.

Supporting Information

Micropillar arrays–enabled single microbial cells encapsulation in hydrogel

Kyun Joo Park, Kyoung G. Lee,* Seunghwan Seok, Bong Gill Choi, Moon-Keun Lee, Tae Jung Park, Jung Youn Park, Do Hyun Kim** and Seok Jae Lee***

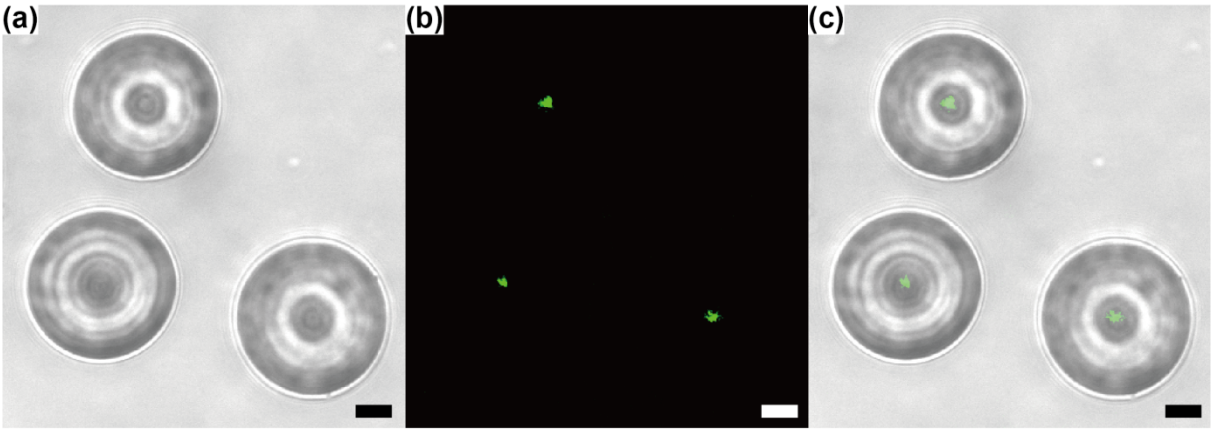

Fig. S1 Encapsulated–*E. coli* cells in the hydrogel microparticles. (a) optical image, (b) confocal fluorescent image, and (c) integration image of (a) and (b). Scale bars represent 10 μm.

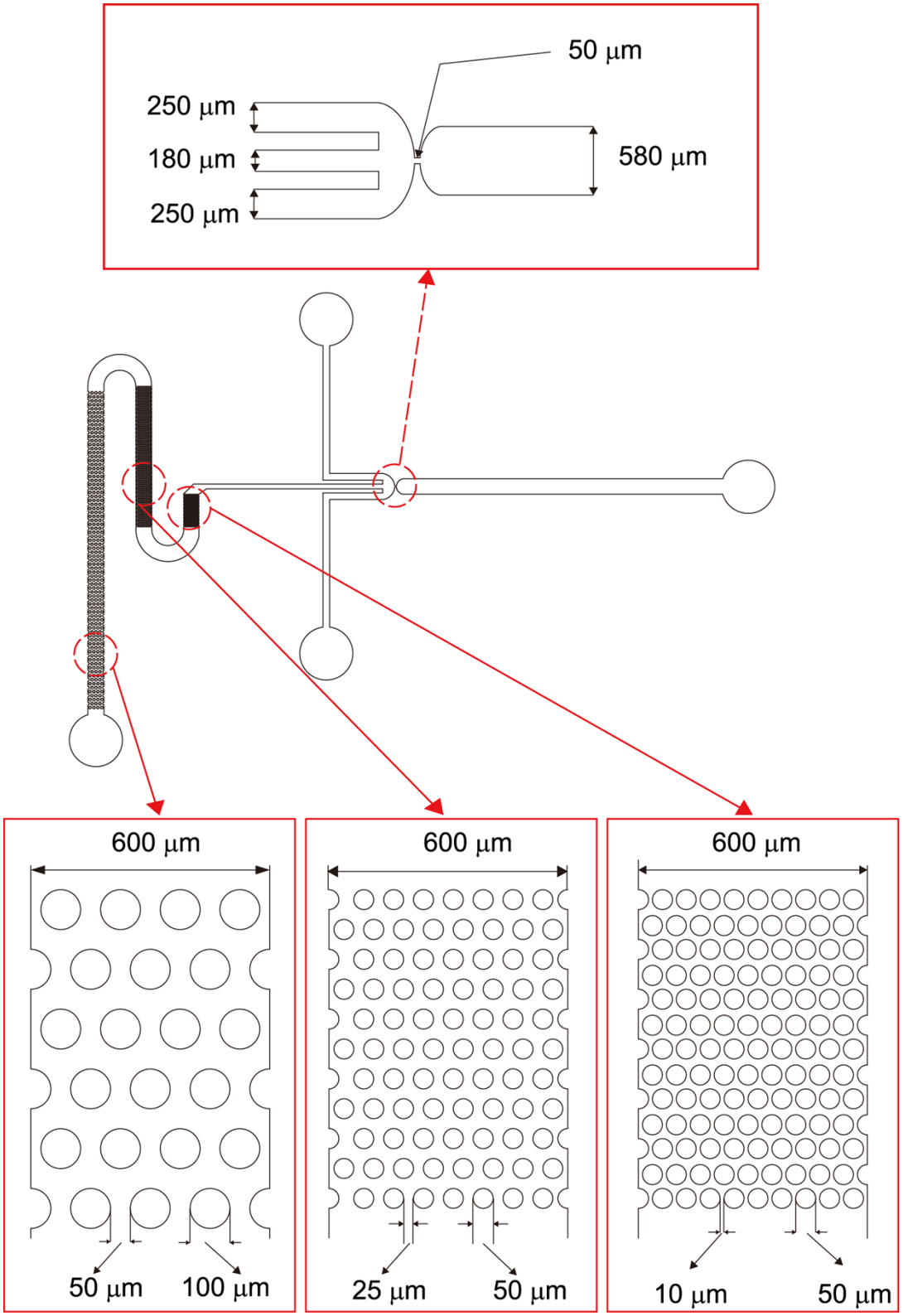

Fig. S2 Schematic illustration of detailed dimensions of microstructure in microfluidic device for fabrication of single–cell encapsulated hydrogel particle.

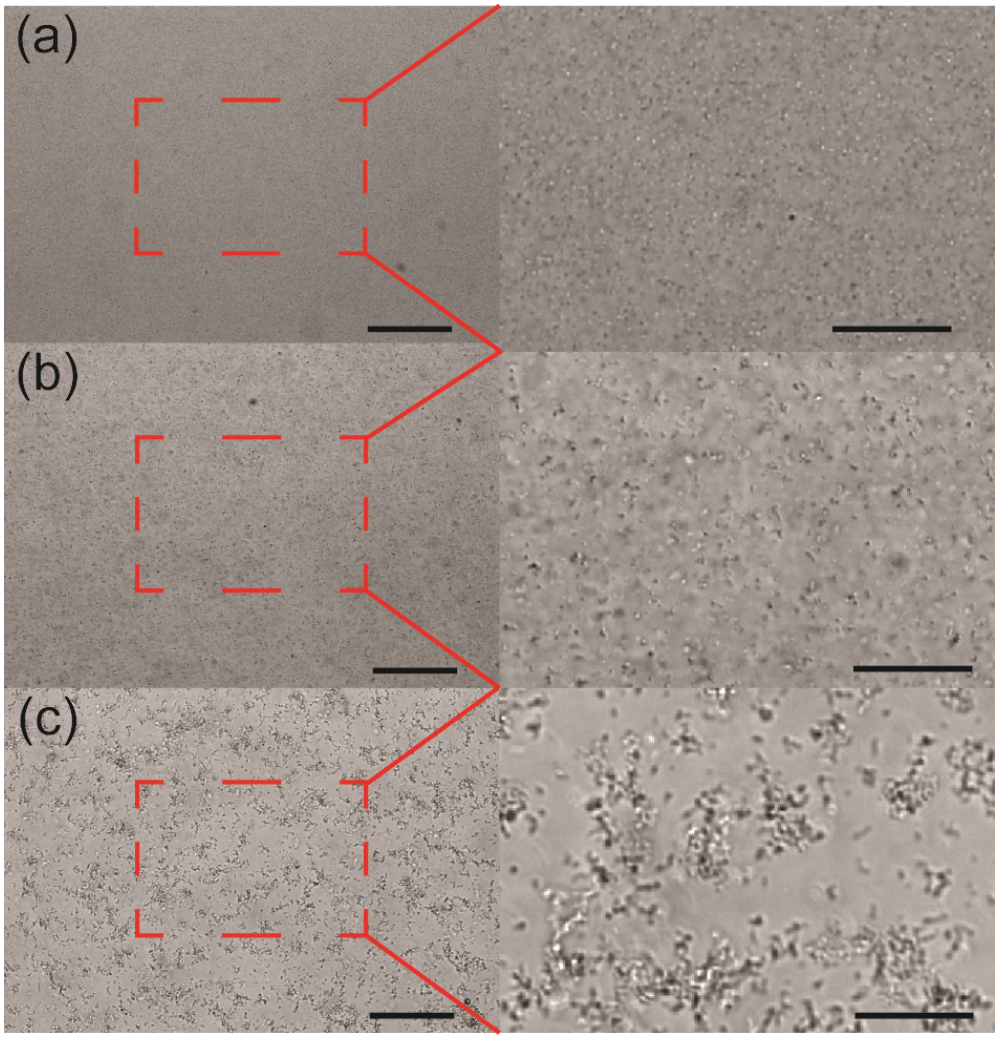

Fig. S3 Microscopic images of cells in LB media and their magnified image of (a) without PEGDA, (b) 13 wt% of PEGDA, and (c) 23 wt% of PEGDA. All the scale bars are 500 μm.

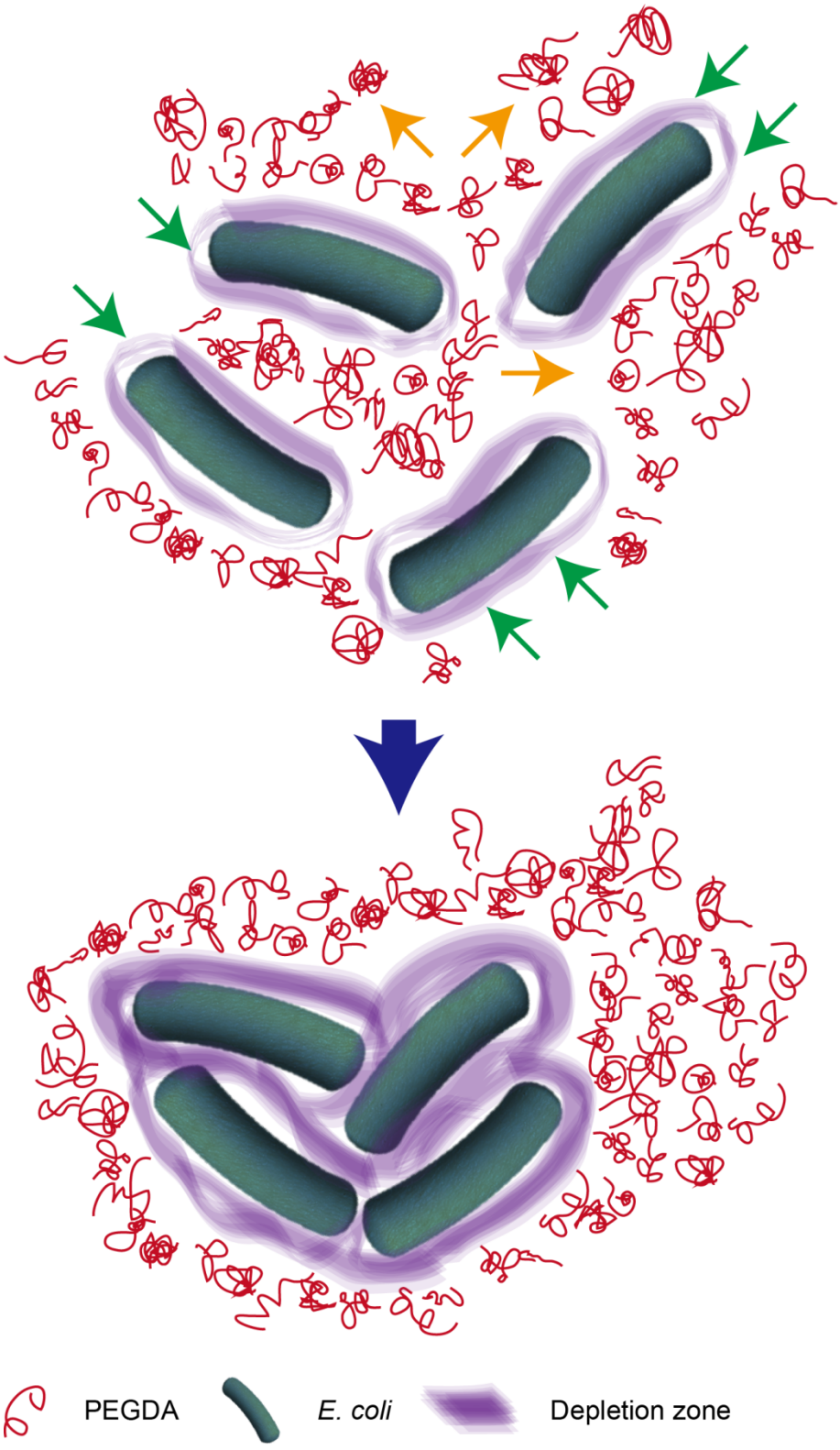

Fig. S4 Schematic illustration of cell aggregation with depleted polymers.

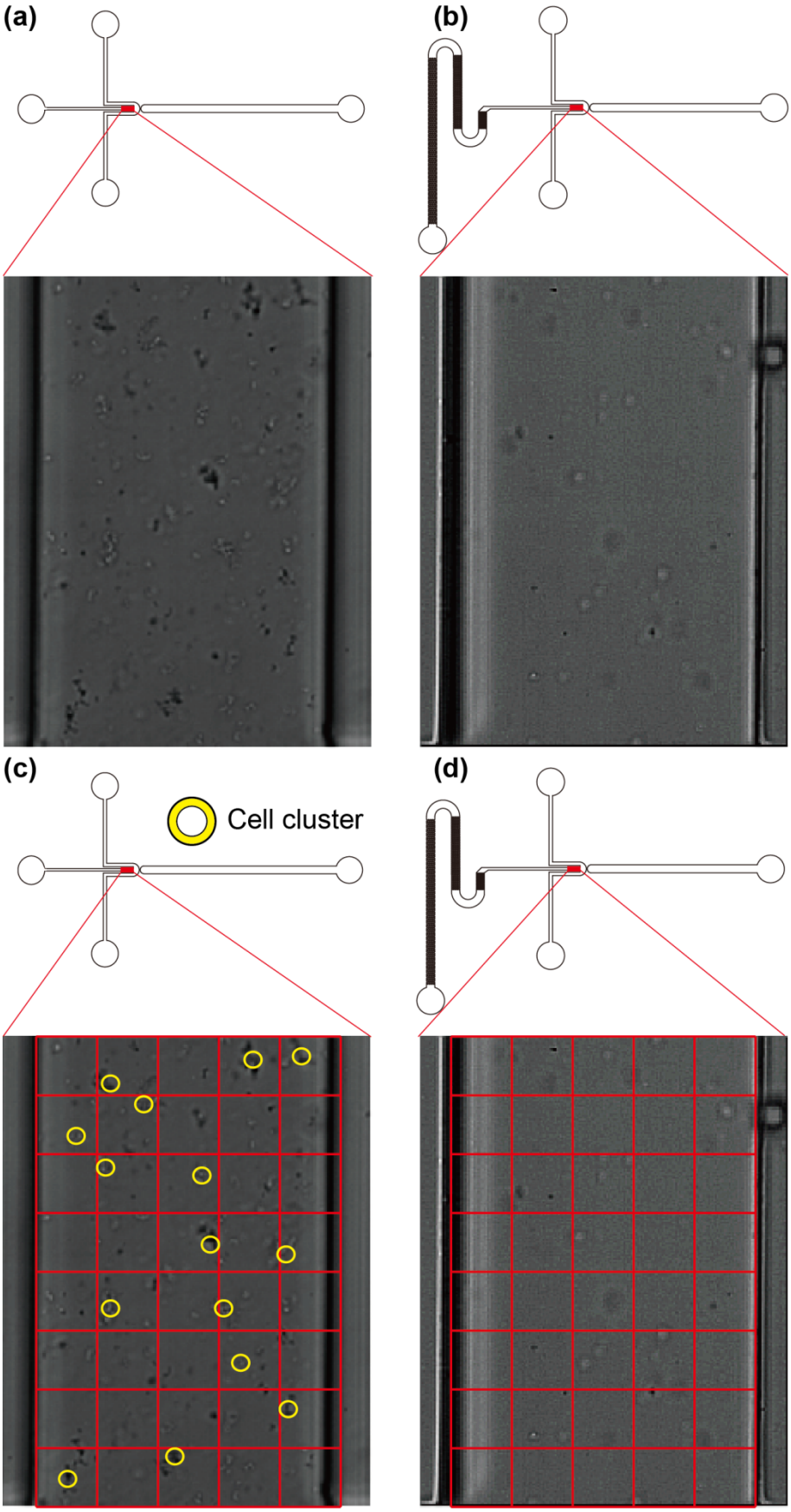

Fig. S5 Microscopic images of cell distribution in microfluidic devices (a) without micropillar arrays, (b) with micropillar arrays and (c-d) processed image of (a-b).

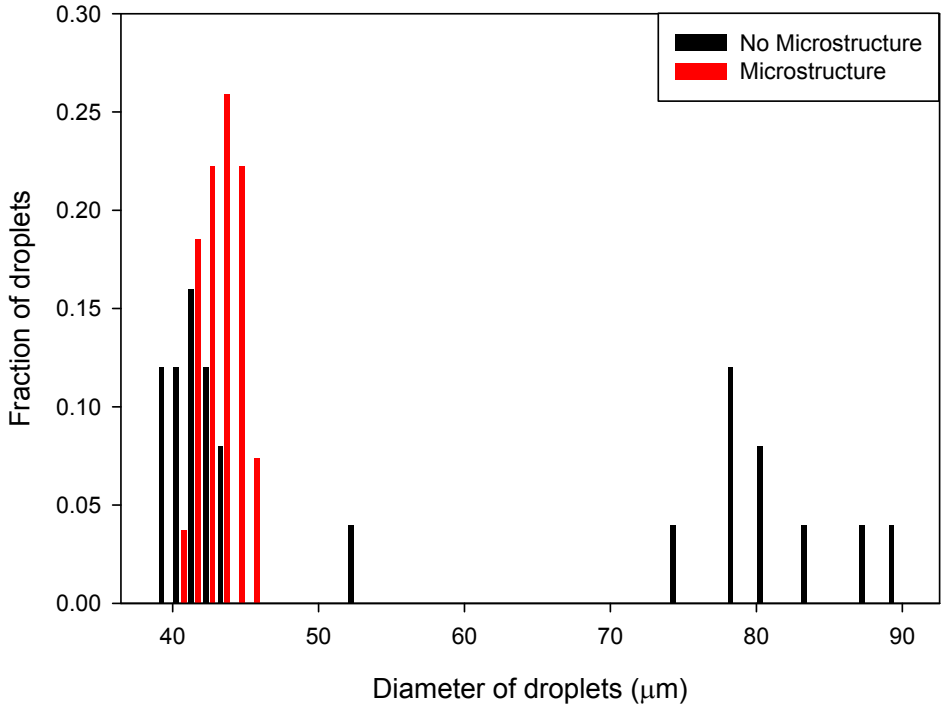

Fig. S6 Droplet size distribution histogram. Each Red and black bars indicate the fraction of droplets using with micropillars and without micropillars, respectively.

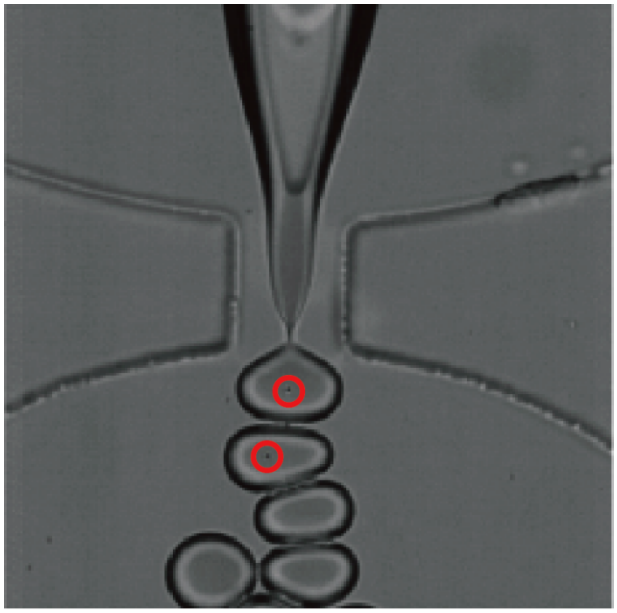

Fig. S7 The image of single–cell encapsulated droplets generation moment at the orifice. The red circles indicate single–cell in the droplets

Table S1 Drag force, collision force, and elongation breakup force with respect to cell-cluster sizes.

Diameter(μm)	F_d [nN]	F_c [nN]	F_e [nN] 1st pillar zone	F_e [nN] 2nd pillar zone	F_e [nN] 3rd pillar zone
2	0.17	1.57×10^{-4}	2.79×10^{-3}	3.99×10^{-3}	7.97×10^{-3}
3	0.26	3.53×10^{-4}	5.83×10^{-3}	8.33×10^{-3}	1.66×10^{-2}
4	0.35	6.28×10^{-4}	9.97×10^{-3}	1.42×10^{-2}	2.84×10^{-2}
5	0.44	9.82×10^{-4}	1.52×10^{-2}	2.17×10^{-2}	4.35×10^{-2}
7.6	0.66	2.27×10^{-3}	0.03	4.85×10^{-2}	9.70×10^{-2}
10	0.87	3.93×10^{-3}	0.06	8.27×10^{-2}	0.17
15	1.31	8.84×10^{-3}	0.13	0.18	–
22.9	1.99	0.02	0.29	0.42	–
38	3.31	0.06	0.80	1.15	–
65	5.66	0.17	1.38	–	–
99	8.62	0.38	–	–	–
152.7	13.31	0.92	–	–	–

Table S2 Cell concentrations corresponded to optical densities at 600 nm.

Optical density (A600)	Number of cells [cells/mL]
0.316	3.16×10^{8}
0.623	6.23×10^{8}
0.752	7.52×10^{8}
0.758	7.58×10^{8}
0.847	8.47×10^{8}
1.707	1.71×10^{9}

The external force calculation

For the better understanding of the mechanisms behind of cell dispersion, the possible theoretical aspects are proposed and discussed. First of all, the drag force, F_d, caused by surrounding fluids guides the cluster to pillar structure and make cluster to pillar collision. This force on the constituent cell is given by the Stokes law as following equation (eqn. S1)[S1]:

$$F_d = 6\pi\mu R V_C \qquad \text{(eqn. S1)}$$

where μ is the viscosity of fluid, R is the radius of dragged material, and V_c is the velocity of the cell. In this case, the viscosity, velocity of cell, and velocity of solution were 6.16 cp, 1.50×10^3 μm/s, and 4.17×10^3 μm/s, respectively. In addition to this, the clusters also stroke with pillars and this collision force is resulted from momentum conservation. The detailed collision force, F_c, is described in the following equation (eqn. S2)

$$F_C = \frac{\Delta P}{\Delta t_C} = m\frac{V_C}{t_C} \qquad \text{(eqn. S2)}$$

Where P represents momentum of cell–cluster, m is mass of cluster, and t_c is the colliding time. The drag force and collision force contribute to the continuous scattering of cell–clusters into small pieces, simultaneously. Overall, the collision and drag forces are initially applied to the clusters. In detail, the collision point of clusters is mainly accounted from conservative momentum to deform their shape and drag force is continuously taken over for the further breaking.

Another important mechanism behind of these phenomena is related to an elongation induced breakup force, $F_{e,}$ when cell–cluster penetrating between micropillars.[36] At this brief moment, the orifice which are made by two pillars, the highest elongation rate are applied by converging flow. It allows continuous breaking and separating of clusters into smaller pieces in the channel. Breakup force of cell–cluster due to converging flow can be obtained by the relationship of the velocity of fluid (V_f), surface area of elongated cluster (S), and the shape of the aggregates (C_{hyd}). The equation is given as following equation (eqn. S3)[S2]

$$F_e = 3^{\frac{3}{2}} \frac{C_{hyd} S \mu V_f}{32 D_H} \quad \text{(eqn. S3)}$$

where D_H is a hydraulic diameter of the orifice. As stepwise narrowing the gap among the pillar zones, the gradual incensement of flow rate leads increase of the elongation force and makes further break–up cell–clusters into single level of cells. The total breakup force, F_B, is simply summarized of combination of F_c, F_d, and F_e as shown in equation (eqn. S4).

$$F_B = F_c + F_d + F_e \quad \text{(eqn. S4)}$$

With these combinations of external forces, the clusters become smaller and smaller then, completely breakup into single–cell level as continuously flowing through the second and third micropillar zone. The forces were calculated using the presented equations as shown in Table S1. The shape of cell–cluster in this calculation is regarded as an ellipsoidal particle.[S3] These combination forces promote and increase the efficiency of micropillars for enhancing the cell dispersion. The obtained force results under different scenarios support among the

proposed mechanisms, the collision and drag force are more dominant compared to the other force because of less elongation generation in the laminar flow.

Reference

[S1] M. M. Denn, in *Process fluid mechanics*, Prentice–Hall, Englewood Cliffs, New Jers ey 1980, Ch. 12, pp. 248-255.

[S2] M. Kobayashi, *Colloids Surf. A,* 2004, **235**, 73-78.

[S3] S. Blaser, *Chem. Eng. Sci*., 2002, **57**, 515-526.